

1  
2  
3  
4  
5  
6  
7  
8  
9  
10  
11  
12  
13  
14  
15  
16  
17  
18  
19  
20  
21  
22  
23  
24  
25  
26  
27  
28

**Muted change in Atlantic overturning circulation over some glacial-aged Heinrich events**

Jean Lynch-Stieglitz<sup>1\*</sup>, Matthew W. Schmidt<sup>2</sup>, L. Gene Henry<sup>1,7</sup>, William B. Curry<sup>3</sup>, Luke C. Skinner<sup>4</sup>, Stefan Mulitza<sup>5</sup>, Rong Zhang<sup>6</sup>, Ping Chang<sup>2</sup>

Submitted to *Nature Geoscience* 9/11/2012

Revised for *Nature Geoscience* 11/11/2013

Published: *Nature Geoscience*. 7: 144-150, 2014. doi: 10.1038/NGEO2045.

<sup>1\*</sup>School of Earth and Atmospheric Sciences, Georgia Institute of Technology, Atlanta, GA, 30307, USA jean@eas.gatech.edu.

<sup>2</sup>Department of Oceanography, Texas A&M University, College Station, TX, 77843, USA.

<sup>3</sup>Woods Hole Oceanographic Institution, Woods Hole, MA 02543, USA.

<sup>4</sup>Godwin Laboratory for Palaeoclimate Research, Department of Earth Sciences, University of Cambridge, Downing Street, Cambridge CB2 3EQ, UK.

<sup>5</sup>MARUM—Center for Marine Environmental Sciences, University of Bremen, Leobener Strasse, D-28359 Bremen, Germany.

<sup>6</sup>NOAA/Geophysical Fluid Dynamics Laboratory, Princeton, NJ 08540, USA

<sup>7</sup>Now at Department of Earth and Environmental Sciences and Lamont-Doherty Earth Observatory of Columbia University, Palisades, NY 10964

29  
30  
31  
32  
33  
34  
35  
36  
37  
38  
39  
40  
41  
42  
43  
44  
45  
46  
47

**Heinrich events - surges of icebergs into the North Atlantic Ocean - punctuated the last glacial period. The events are associated with millennial-scale cooling in the Northern Hemisphere. Freshwater from the melting icebergs is thought to have interrupted the Atlantic meridional overturning circulation, thus minimizing heat transport into the northern North Atlantic. The northward flow of warm water passes through the Florida Straits and is reflected in the distribution of seawater properties in this region. Here we investigate the northward flow through this region over the past 40,000 years using oxygen isotope measurements of benthic foraminifera from two cores on either side of the Florida Straits, which allow us to estimate water density, which is related to flow via the thermal wind relation. We infer a substantial reduction of flow during Heinrich Event 1 and the Heinrich-like Younger Dryas cooling, but little change during Heinrich Events 2 and 3, which occurred during an especially cold phase of the last glacial period. We speculate that because glacial circulation was already weakened before the onset of Heinrich Events 2 and 3, freshwater forcing had little additional effect. However, low-latitude climate perturbations were observed during all events. We therefore suggest these perturbations may not have been directly caused by changes in heat transport associated with Atlantic overturning circulation as commonly assumed.**

48           Layers of ice rafted debris, Heinrich layers, appear periodically in the sediments of the  
49 North Atlantic that were laid down during the last glacial period. These layers are thought to  
50 represent surges of the large continental ice sheet that covered North America, discharging fresh  
51 water in the form of debris laden ice into the North Atlantic. The input of freshwater into the

52 North Atlantic is postulated to have disrupted deep and bottom water formation, leading to a  
53 weaker Atlantic Meridional Overturning Circulation (AMOC).

54 The times surrounding the Heinrich Events (Heinrich Stadials) are clearly marked by  
55 extreme conditions in many records of oceanic and climatic change far from the North Atlantic.  
56 These stadials are associated with drier than normal conditions in China<sup>1</sup> and the Sahel<sup>2</sup>, and  
57 reduced ventilation of intermediate waters in the Arabian Sea<sup>3</sup>. Some Heinrich stadials are  
58 marked by warming of both the ocean and climate in the southern hemisphere<sup>4</sup>. It is thought that  
59 many of these far field effects of the ice discharges are transmitted by changes in the AMOC  
60 driven heat transport from the southern to the northern hemisphere, and the associated changes in  
61 atmospheric and oceanic circulation. If this were the case, we would expect to see evidence for  
62 changes in AMOC for each of the Heinrich Stadials.

63

#### 64 **Expression of Heinrich Stadials in existing records of past ocean circulation**

65 Reconstructions of the water mass properties in the Atlantic during glacial times have  
66 yielded a picture of a nutrient poor water mass (Glacial North Atlantic Intermediate Water,  
67 GNAIW), overlying a nutrient rich water mass, presumably sourced from the south<sup>5</sup>.

68 Reconstructions of the density gradient in the upper ocean and model-data comparisons with  
69 deep water carbon isotope data suggest that if this configuration was associated with a shallower  
70 AMOC, this circulation was quite a bit weaker than the present day<sup>6-8</sup>. However, a recent  
71 model-data comparison suggests that sedimentary Pa and Th data are consistent with a strong,  
72 shallow AMOC<sup>9</sup>.

73 It has been suggested that during Heinrich Stadials, this shallower AMOC was disrupted  
74 by freshwater input to the North Atlantic, leading to a virtual shutdown in the AMOC<sup>10</sup>. This

75 idea was based on both ocean general circulation models which showed such a response to a  
76 large freshwater input, and data which suggested high nutrient values<sup>11</sup> in deep waters around the  
77 time the most recent Heinrich layer (H1) was deposited. The idea of a weakened or non-existent  
78 overturning associated with H1 was bolstered by the discovery that the ratio of the particle  
79 reactive decay products of U, <sup>231</sup>Pa and <sup>230</sup>Th are buried in the same ratio at which they are  
80 produced in the overlying water column in the open North Atlantic<sup>12</sup>.

81 Evidence for circulation changes associated with the Heinrich Events other than H1 has  
82 remained equivocal. The Pa and Th in deep Atlantic sediments do show a higher ratio during the  
83 stadials associated with H2 and H3, but these higher ratios are accompanied by evidence for an  
84 increase in opal flux to the seafloor, so may not necessarily indicate a circulation change<sup>13</sup>.

85 Despite extensive efforts to reconstruct changes in water mass properties in the North Atlantic  
86 using carbon isotopic and trace metal measurements in the calcite tests of foraminifera, these  
87 records also do not show a clear picture of water mass changes for earlier Heinrich Events. This  
88 work is often hampered by poor time resolution and noisy data, perhaps due to productivity  
89 overprints<sup>14</sup>. Some records suggest the presence of nutrient rich waters at intermediate (<2 km)  
90 depths during some of the Heinrich Stadials but not others<sup>15-20</sup>. However, the response is  
91 inconsistent among different locations in these upper water masses, suggesting that regional  
92 changes in productivity or circulation may have been responsible for these excursions towards  
93 more nutrient rich values. Deep water (> 2 km) records show clear excursions towards a more  
94 nutrient-rich water mass during the stadials associated with H4 and H5 but not all records show  
95 changes around the time of H2 or H3 when deep water nutrient concentrations are already high  
96 (Supplemental Figures 1, 2). However, the link between the extent of the high and low nutrient  
97 water masses and circulation is indirect. It is possible that despite changes in circulation, a core

98 site is bathed by the same water mass and this circulation change is not reflected in the nutrient  
99 status at this core site. Similarly, if the change in circulation persists for only a short period of  
100 time, the chemical properties of the deep water might not fully reflect the changes for several  
101 hundred years.

102 Here we present time-series of the oxygen isotopic composition of benthic foraminifera  
103 from the Florida Straits which we believe to be sensitive to changes in the upper branch of the  
104 AMOC, and the carbon isotopic composition of benthic foraminifera from the same region which  
105 can be used to reconstruct the nutrient concentration of intermediate waters. We use these  
106 records, together with existing reconstructions from other sites, to argue that if any reductions in  
107 the AMOC accompanied the two Heinrich Events that occurred during full glacial conditions  
108 (H2, H3), they were of a much smaller magnitude and/or shorter duration than the reductions  
109 occurring during H1 and the Younger Dryas.

110

### 111 **Expression of Heinrich Stadials 1, 2 and 3 in the Florida Straits**

112 As it flows through the Florida Straits, the strength of the Florida Current reflects both  
113 the western limb of wind driven subtropical gyre and the warm surface waters that cross the  
114 equator and travel to the North Atlantic as part of the upper branch of the large scale overturning  
115 circulation associated with deep water formation. Any change in either this large scale  
116 overturning or wind driven gyre circulation can change the strength of this current. To first  
117 order, this current is in geostrophic balance so the vertical shear in the flow is proportional to the  
118 horizontal density gradient across the Straits. The density gradient at times in the past can be  
119 inferred from the oxygen isotopic composition of the calcite tests of benthic foraminifera from  
120 sediment cores on both sides of the current. The oxygen isotope ratio reflects both the

121 temperature and oxygen isotopic composition (related to salinity) of the seawater in which it  
122 forms, and is therefore related to seawater density. Using this approach we have shown that the  
123 cross strait gradient was reduced during both the Last Glacial Maximum<sup>7</sup> and the Younger  
124 Dryas<sup>21</sup>. The reduced gradient can be explained by a reduction in the strength of the AMOC  
125 during the Last Glacial Maximum and Younger Dryas relative to the modern state, consistent  
126 with inferences based on other paleoceanographic studies using different methods.

127         While it is not possible to exclude the possibility that a reduced cross strait gradient  
128 reflected a reduced wind driven flow or a more barotropic Florida current, we do show that the  
129 link among AMOC strength, Florida Current strength and cross strait density gradient holds in a  
130 previously published model experiment (Supplemental Figure 5). In this model experiment, an  
131 AMOC reduction of ~11 Sv was induced in CCSM by freshwater input into the subpolar North  
132 Atlantic under LGM conditions<sup>24</sup>. This AMOC reduction was accompanied by a reduction in  
133 Florida Straits transport of ~10 Sv, and a reduction in the cross straits density gradient at all  
134 depths below 300 m. Details on the model experiment can be found in the Methods Section.

135         In this paper we show isotopic data from two cores on either side of the Florida Straits  
136 (KNR166-2-26JPC, 24° 19.61'N, 83° 15.14'W, 546 m, KNR166-2-73GGC, 23° 44.73'N, 79°  
137 25.78'S, 542 m, Figure 1). Details on the methods including age model development and  
138 isotopic measurements can be found in the Methods Section. The core on the Florida Margin  
139 extends through 36 kyr before present, has high sedimentation rates (15-35 cm kyr<sup>-1</sup>) during  
140 Marine Isotope Stages 2 and 3, and should be able to resolve changes associated with Heinrich  
141 Events during this interval. This core shows prominent excursions towards lower  $\delta^{18}\text{O}$  values  
142 (warmer or less saline, less dense waters) during the Younger Dryas and around the time the  
143 most recent Heinrich Event (Heinrich Stadial 1, HS1) (Figure 2a). The Younger Dryas excursion

144 is associated with a reduction in cross strait  $\delta^{18}\text{O}$  gradient as inferred from three sediment cores  
145 on each side of the Straits (ref<sup>21</sup>). Due to the low sedimentation rates between 13-20 kyr on the  
146 Bahamas side of the straits, we have no direct evidence that the HS1 excursion was similarly  
147 associated with a reduction in the cross strait density gradient. However, by analogy to the YD  
148 excursion, such a reduction certainly seems plausible.

149 More generally, many general circulation models show mid-depth warming in the  
150 subtropical North Atlantic when the AMOC is weakened in water hosing experiments in which  
151 extra freshwater forcing is distributed over the northern North Atlantic.<sup>22</sup> The warming is often  
152 particularly apparent along the western margin of the subtropical North Atlantic<sup>23,24</sup>. As an  
153 example, we show the mid-depth temperature anomaly from the model experiment with the 11  
154 Sv freshwater-induced AMOC reduction described above (Figure 3). There is a positive mid-  
155 depth temperature anomaly associated with the AMOC weakening along the entire western  
156 margin of the basin. The mechanisms for this western margin warming are likely multiple and  
157 linked, involving the dynamic adjustment of the density structure in association with the  
158 circulation change, decreased heat transport out of the subtropics into the mid-latitude North  
159 Atlantic, and a decreased contribution of the relatively cooler and fresher intermediate waters  
160 from the South Atlantic.<sup>24,25</sup> In light of the results from these models, the negative excursion in  
161 benthic foraminiferal  $\delta^{18}\text{O}$  along the Florida Margin, even in the absence of information about  
162 the cross-strait density gradient, supports the scenario of an AMOC reduction during HS1. In the  
163 model study shown in Figure 3, an AMOC reduction of 11 Sv was associated with an increase in  
164 temperature at 550m water depth along the South Florida Margin of 1.8°C, which all else being  
165 equal would correspond to a  $\delta^{18}\text{O}$  change in benthic foraminifera at this site of about -0.5 ‰, the  
166 same magnitude that is observed for HS1. There was only a small (< 0.1 psu) salinity anomaly at

167 this location associated with the weakened AMOC. Regardless of the dominant process, an  
168 interpretation of the excursion towards lower  $\delta^{18}\text{O}$  at the Florida Margin as reflecting a reduced  
169 AMOC is consistent with the multiple lines of evidence for such a reduction during HS1 (ref.  
170 <sup>11,12</sup>).

171 In contrast, there is no indication of a significant change in cross-strait  $\delta^{18}\text{O}$  for the  
172 stadials associated with Heinrich events 2 and 3 (HS2, HS3). However the resolution of the  
173 Bahamas core may be insufficient to capture a short-lived reduction in the cross-strait gradient.  
174 But we do not see excursions towards lower benthic  $\delta^{18}\text{O}$  values similar in magnitude to that  
175 observed for the Younger Dryas and HS1 in the much higher resolution Florida core for HS2 or  
176 HS3. It is possible that competing processes (e.g. water mass property changes of the opposite  
177 sign which exactly matched in magnitude the changes associated with the flattening of  
178 isopycnals across the Florida Current, or a strengthening of the wind driven flow compensating a  
179 weakening of the AMOC) lead to a very muted or non-existent change in  $\delta^{18}\text{O}$  at this site, despite  
180 significant changes in the AMOC. However, it seems more reasonable to conclude, especially in  
181 light of the lack of compelling evidence for changes in the properties or extent of the deep  
182 Atlantic water masses during these Heinrich Stadials, that any changes in the AMOC in response  
183 to these two Heinrich Events were not comparable in size to the changes observed for the  
184 Younger Dryas or HS1. While the YD and HS1 are almost always associated with excursions in  
185 deep Atlantic  $\delta^{13}\text{C}$  (a proxy for nutrient content and water mass ventilation), similarly coherent  
186 excursions are not observed for HS2 and HS3 (Figure 2b, Supplemental Figure 2). While it is  
187 possible that the nutrient tracers would not fully respond to a very short duration change in ocean  
188 circulation, the upper ocean density structure, and thus the  $\delta^{18}\text{O}$  of foraminifera on the Florida  
189 Margin, would adjust very quickly to reflect a different flow state.



190 It is perhaps unsurprising that H3 may not be associated with dramatic circulation  
191 changes. The sediments in this Heinrich layer are geochemically distinct from the others, it often  
192 shows up as a smaller peak in the concentration of ice rafted debris in sediment cores, and it is  
193 limited to a smaller area in the North Atlantic than the other events<sup>26</sup>. It is certainly plausible that  
194 a smaller volume of melt water, or the discharge of melt water into a different region within the  
195 North Atlantic, could explain the lack of interruption of the AMOC. However, H2 appears  
196 robust and geochemically similar to the events that do appear to be associated with circulation  
197 changes (H1, H4, H5). The lack of a large circulation change associated with H2 would  
198 therefore require a different explanation.

199

#### 200 **Response of ocean circulation to freshwater input sensitive to circulation state**

201 The earlier Heinrich events (H4, H5) appear at a time (~33- 60 kyr ago, Early MIS Stage  
202 3) when the contrast between deep and intermediate  $\delta^{13}\text{C}$  values was not as extreme as during the  
203 full glacial state (Figure 4d). The excursions in deepwater  $\delta^{13}\text{C}$  at the time of these earlier H  
204 events seem to reflect transitions from more weak stratification in the geochemical water mass  
205 properties (modern type, associated with strong AMOC today), to the more strongly stratified  
206 LGM water mass configuration which is associated with a weaker AMOC (Figure 5). The  
207 Younger Dryas AMOC weakening is also thought to be melt water induced, and like HS4 and  
208 HS5 seems to reflect a transition from a modern water mass configuration to one more similar to  
209 the glacial state<sup>27</sup>.

210 We postulate that since the circulation was already in this more geochemically stratified,  
211 weakened glacial state for the interval encompassing H2 and H3, the freshwater discharge  
212 associated with these events was not able to weaken the AMOC further. This result apparently

213 contradicts ocean general circulation model studies suggesting that a given freshwater input has a  
214 stronger impact on AMOC strength in the glacial climate state than the modern state<sup>28-30</sup>.  
215 Heinrich Event 1 also occurs during full glacial time, but the circulation event that is associated  
216 with it seems particularly long and intense, lasting several thousand years, starting around the  
217 time of the ice rafting event (16.8 kyr BP, ref. <sup>26</sup>) and persisting well into the deglaciation until  
218 about 14.7 kyr BP (Figure 2)<sup>12</sup>. It is possible that the additional melt water entering the North  
219 Atlantic as the Northern Hemisphere Ice Sheets began to decay helped to develop and sustain the  
220 circulation change beyond the time of the Heinrich Event.

221         If the ice sheet surges only significantly impact the AMOC for some of the H events, this  
222 has implications for the mechanisms responsible for the global expression of the H events. There  
223 are some well resolved paleoclimate records in the Northern Hemisphere that suggest strong  
224 changes in atmospheric circulation for all of the Heinrich stadials, including HS2 and HS3  
225 (Figure 4). These include records of the Asian Monsoon from China<sup>1</sup> and the ITCZ/monsoon  
226 areas of the tropical Atlantic<sup>2,31</sup> and ventilation in the Arabian Sea<sup>3</sup>. While changes in the heat  
227 transport associated with the AMOC can change the position of the Atlantic ITCZ<sup>23</sup>, if there were  
228 no, or only very subtle, changes in the AMOC over HS2 and HS3, a mechanism involving  
229 atmospheric transmission is needed to explain the large signals for both the “circulation H  
230 events” (H1, H4, H5, H6) and the H events that occur during peak glacial times (H2, H3). More  
231 generally, cooling and increased land or sea ice cover in North Atlantic has also been shown to  
232 cause shifts in the ITCZ<sup>32,33</sup>, providing a potential mechanism for ITCZ changes not directly  
233 linked to the AMOC. Shifts in the Northern Hemisphere planetary wave patterns in response to  
234 either North Atlantic sea ice extent or changes in ice sheet height<sup>34</sup> might also provide a link

235 between the H events in the North Atlantic and these lower latitude indicators of atmospheric  
236 change.

237

## 238 **Methods**

239 Core KNR166-2-26JPC was taken from a water depth of 546 m on the Florida Margin  
240 and KNR166-2-73GGC was from a water depth of 542 m in the Santaren Channel (Bahamas).  
241 The age models for both cores were developed by linear interpolation between radiocarbon dates  
242 converted to calendar years using Calib 6.0 and the MARINE09 calibration data set<sup>35</sup>. In  
243 addition to the radiocarbon dates, the ages of Marine Isotope Stage 3 – 4 and 4 - 5 boundaries  
244 were used to refine the age model for KNR166-2-73GGC (Supplemental Table 1). For  
245 KNR162-2-26JPC the out of sequence dates between 344 and 408 cm were not used in the age  
246 model as was discussed in a previous publication on the deglacial portion of this core<sup>21</sup>. In  
247 addition we do not use the date at 1032.25 cm depth due to the large error in the radiocarbon  
248 measurement or the out of sequence date at 1088.25 cm.

249 For core KNR166-2-26JPC both small single species groups (up to 4 individuals) and  
250 individuals of *Planulina ariminensis*, *Cibicidoides pachyderma* and *Cibicidoides mollis* from the  
251 size fraction >250  $\mu\text{m}$  were analyzed for oxygen and carbon isotopes. Isotope measurements  
252 were made on a GV Instruments Optima with Multiprep at the Lamont-Doherty Earth  
253 Observatory and a Finnigan MAT253 with Kiel carbonate preparation device at the Georgia  
254 Institute of Technology. Values were calibrated using NBS-19 and NBS-18, and in all labs  
255 internal precision met or exceeded 0.08‰ (1 sigma s.d. of replicate analyses of NBS-19 or in  
256 house standards). We then averaged the  $\delta^{18}\text{O}$  values for all species at each depth interval, with  
257 an average of 5 individuals contributing to the average value at each depth. A small number of

258 measurements show very low  $\delta^{18}\text{O}$  values, and presumably represent individuals that were  
259 transported down slope from shallower water depths. The values that were greater than two  
260 standard deviations away from a robust loess smoothed version of the record were flagged (4%  
261 of the data) and not included in the average  $\delta^{18}\text{O}$  calculated for each depth (Supplemental Figure  
262 4). The average value for each depth (outliers removed as described above) and the robust loess  
263 smooth are shown in Figure 2a. For the carbon isotope data shown in Figure 2b and Figure 4d,  
264 only the data from *P. ariminensis* are averaged at each depth, as the  $\delta^{13}\text{C}$  values of the other  
265 species are consistently lower suggesting a phytodetritus effect at this location (Supplemental  
266 Figure 4). Most data from the portion of the core younger than 15,000 ka BP was previously  
267 published<sup>21</sup>.

268 For core KNR166-2-73JPC individuals of *P. ariminensis* and *C. pachyderma* from the  
269 size fraction  $>250\ \mu\text{m}$  were analyzed for oxygen and carbon isotopes. Isotope measurements  
270 were made on a Finnigan MAT253 with Kiel carbonate preparation device at Georgia Institute of  
271 Technology. We averaged the  $\delta^{18}\text{O}$  values for all species at each depth interval, with between 1-  
272 3 individuals contributing to the average value at each depth. For the  $\delta^{13}\text{C}$  record shown in  
273 Figure 3d, only values from *C. pachyderma* are averaged, since analyses for this species were  
274 available for the entire length of the record. Where both species are analyzed in the Holocene  
275 portion of the record, the  $\delta^{13}\text{C}$  of *C. pachyderma* is about 0.2‰ lower than *P. ariminensis*.

276 The age model for the *N. pachyderma*  $\delta^{18}\text{O}$  record for MD95-2024P<sup>36</sup> (Figure 4a) was  
277 constructed by correlating the detrital layers in this core to the dates of the Heinrich Stadials in  
278 the Hulu Cave oxygen isotope record<sup>1</sup>. The original age model for this core was determined in a  
279 similar manner by correlating the detrital layers to the cold stadials in the Greenland ice core

280 record<sup>37</sup>. All other data sets plotted in Figure 4 are shown on their original published age  
281 models.

282 The water hosing experiment shown in Figure 3b was performed using the Community  
283 Climate System Model, version 3.0, a fully coupled ocean-atmosphere global circulation model  
284 developed at NCAR. The model experiment was initialized at year 400 of a control run under  
285 LGM climate boundary conditions. Extra freshwater forcing of 0.25 Sv was uniformly  
286 distributed over the subpolar North Atlantic (50°–70°N) for the 100 yr duration of the  
287 experiment. The maximum overturning weakens from 17 Sv in the LGM control run to 6 Sv in  
288 the last 30 years of the experiment. The Florida Straits transport is well simulated in this model  
289 and weakens from 33 Sv in the control run to 23 Sv in the experiment. This weakening is  
290 accompanied by a decrease in the density gradient across the Florida Straits as all depths below  
291 300 m (Supplemental Figure 5). Further details on the model and experiment can be found in the  
292 original publication<sup>24</sup>.

### 293 *Data*

294 All radiocarbon dates and isotope data reported in this study are archived at World Data  
295 Center-A for Paleoclimatology located at the U.S. National Oceanic and Atmospheric  
296 Administration (NOAA) National Climatic Data Center (NCDC) Paleoclimatology Program,  
297 Boulder, Colorado.

298

299

300

301 **References**

302

303 1 Wang, Y. J. *et al.* A high-resolution absolute-dated Late Pleistocene monsoon record from Hulu Cave,  
304 China. *Science* **294**, 2345-2348 (2001).

305 2 Mulitza, S. *et al.* Sahel megadroughts triggered by glacial slowdowns of Atlantic meridional overturning.  
306 *Paleoceanography* **23**, PA4206, doi:Doi 10.1029/2008pa001637 (2008).

307 3 Schulz, H., von Rad, U. & Erlenkeuser, H. Correlation between Arabian Sea and Greenland climate  
308 oscillations of the past 110,000 years. *Nature* **393**, 54-57 (1998).

309 4 Blunier, T. & Brook, E. J. Timing of millennial-scale climate change in Antarctica and Greenland during  
310 the last glacial period. *Science* **291**, 109-112 (2001).

311 5 Lynch-Stieglitz, J. *et al.* Atlantic meridional overturning circulation during the Last Glacial Maximum.  
312 *Science* **316**, 66-69 (2007).

313 6 Lynch-Stieglitz, J. *et al.* Meridional overturning circulation in the South Atlantic at the last glacial  
314 maximum. *Geochem Geophys Geosy* **7**, Q10N03, doi:10.1029/2005GC001226 (2006).

315 7 Lynch-Stieglitz, J., Curry, W. B. & Slowey, N. Weaker Gulf Stream in the Florida Straits during the Last  
316 Glacial Maximum. *Nature* **402**, 644-648 (1999).

317 8 Hesse, T., Butzin, M., Bickert, T. & Lohmann, G. A model-data comparison of delta C-13 in the glacial  
318 Atlantic Ocean. *Paleoceanography* **26**, doi:10.1029/2010pa002085 (2011).

319 9 Lippold, J. *et al.* Strength and geometry of the glacial Atlantic Meridional Overturning Circulation. *Nature*  
320 *Geoscience* **5**, 813-816, doi:Doi 10.1038/Ngeo1608 (2012).

321 10 Rahmstorf, S. Ocean circulation and climate during the past 120,000 years. *Nature* **419**, 207-214 (2002).

322 11 Sarnthein, M. *et al.* Changes in East Atlantic Deep-Water Circulation Over the Last 30,000 Years - 8 Time  
323 Slice Reconstructions. *Paleoceanography* **9**, 209-267 (1994).

324 12 McManus, J. F., Francois, R., Gherardi, J. M., Keigwin, L. D. & Brown-Leger, S. Collapse and rapid  
325 resumption of Atlantic meridional circulation linked to deglacial climate changes. *Nature* **428**, 834-837  
326 (2004).

327 13 Lippold, J. *et al.* Does sedimentary (231)Pa/(230)Th from the Bermuda Rise monitor past Atlantic  
328 Meridional Overturning Circulation? *Geophysical Research Letters* **36**, doi:10.1029/2009GL038068  
329 (2009).

330 14 Boyle, E. A. Is ocean thermohaline circulation linked to abrupt stadial/interstadial transitions? *Quaternary*  
331 *Science Reviews* **19**, 255-272 (2000).

332 15 Zahn, R. *et al.* Thermohaline instability in the North Atlantic during meltwater events: Stable isotope and  
333 ice-rafted detritus records from core SO75-26KL, Portuguese Margin. *Paleoceanography* **12**, 696-710  
334 (1997).

335 16 Peck, V. L., Hall, I. R., Zahn, R. & Scourse, J. D. Progressive reduction in NE Atlantic intermediate water  
336 ventilation prior to Heinrich events: Response to NW European ice sheet instabilities? *Geochem Geophys*  
337 *Geosy* **8**, -, doi:10.1029/2006gc001321 (2007).

338 17 Oppo, D. W. & Lehman, S. J. Suborbital Timescale Variability of North-Atlantic Deep-Water During the  
339 Past 200,000 Years. *Paleoceanography* **10**, 901-910 (1995).

340 18 van Kreveld, S. *et al.* Potential links between surging ice sheets, circulation changes, and the Dansgaard-  
341 Oeschger cycles in the Irminger Sea, 60-18 kyr. *Paleoceanography* **15**, 425-442 (2000).

342 19 Voelker, A. H. L. *et al.* Mediterranean outflow strengthening during northern hemisphere coolings: A salt  
343 source for the glacial Atlantic? *Earth and Planetary Science Letters* **245**, 39-55, doi:Doi  
344 10.1016/J.epsl.2006.03.014 (2006).

345 20 Curry, W. B., Marchitto, T. M., McManus, J. F., Oppo, D. W. & Laarkamp, K. L. in *Mechanisms of Global*  
346 *Climate Change at Millennial Time Scales* Vol. 112 *Geophysical Monograph* (eds PU Clark, RS Webb, &  
347 LD Keigwin) 59-76 (American Geophysical Union, 1999).

348 21 Lynch-Stieglitz, J., Schmidt, M. W. & Curry, W. B. Evidence from the Florida Straits for Younger Dryas  
349 ocean circulation changes. *Paleoceanography* **26**, doi:10.1029/2010PA002032 (2011).

350 22 Stouffer, R. J. *et al.* Investigating the causes of the response of the thermohaline circulation to past and  
351 future climate changes. *Journal of Climate* **19**, 1365-1387, doi:Doi 10.1175/Jcli3689.1 (2006).

352 23 Zhang, R. & Delworth, T. L. Simulated tropical response to a substantial weakening of the Atlantic  
353 thermohaline circulation. *Journal of Climate* **18**, 1853-1860 (2005).

354 24 Schmidt, M. W. *et al.* Impact of abrupt deglacial climate change on tropical Atlantic subsurface  
355 temperatures. *Proceedings of the National Academy of Sciences of the United States of America* **109**,  
356 14348-14352, doi:Doi 10.1073/Pnas.1207806109 (2012).

357 25 Chang, P. *et al.* Oceanic link between abrupt changes in the North Atlantic Ocean and the African  
358 monsoon. *Nature Geoscience* **1**, 444-448, doi:Doi 10.1038/Ngeo218 (2008).

359 26 Hemming, S. R. Heinrich events: Massive late pleistocene detritus layers of the North Atlantic and their  
360 global climate imprint. *Reviews of Geophysics* **42**, -, doi:10.1029/2003rg000128 (2004).

361 27 Keigwin, L. D. Radiocarbon and stable isotope constraints on Last Glacial Maximum and Younger Dryas  
362 ventilation in the western North Atlantic. *Paleoceanography* **19**, doi:10.1029/2004PA001029 (2004).

363 28 Bitz, C. M., Chiang, J. C. H., Cheng, W. & Barsugli, J. J. Rates of thermohaline recovery from freshwater  
364 pulses in modern, Last Glacial Maximum, and greenhouse warming climates. *Geophysical Research*  
365 *Letters* **34**, -, doi:10.1029/2006GL029237 (2007).

366 29 Weber, S. L. & Drijfhout, S. S. Stability of the Atlantic meridional overturning circulation in the last glacial  
367 maximum climate. *Geophysical Research Letters* **34**, -, doi:10.1029/2007gl031437 (2007).

368 30 Swingedouw, D. *et al.* Impact of Freshwater Release in the North Atlantic under Different Climate  
369 Conditions in an OAGCM. *Journal of Climate* **22**, 6377-6403, doi:Doi 10.1175/2009jcli3028.1 (2009).

370 31 Arz, H. W., Patzold, J. & Wefer, G. Correlated millennial-scale changes in surface hydrography and  
371 terrigenous sediment yield inferred from last-glacial marine deposits off northeastern Brazil. *Quaternary*  
372 *Research* **50**, 157-166 (1998).

373 32 Broccoli, A. J., Dahl, K. A. & Stouffer, R. J. Response of the ITCZ to Northern Hemisphere cooling.  
374 *Geophysical Research Letters* **33**, -, doi:10.1029/2005GL024546 (2006).

375 33 Chiang, J. C. H., Biasutti, M. & Battisti, D. S. Sensitivity of the Atlantic Intertropical Convergence Zone to  
376 Last Glacial Maximum boundary conditions. *Paleoceanography* **18**, -, doi:10.1029/2003PA000916 (2003).

377 34 Wunsch, C. Abrupt climate change: An alternative view. *Quaternary Research* **65**, 191-203 (2006).

378 35 Reimer, P. J. *et al.* Intcal09 and Marine09 Radiocarbon Age Calibration Curves, 0-50,000 Years Cal Bp.  
379 *Radiocarbon* **51**, 1111-1150 (2009).

380 36 Hillaire-Marcel, C. & Bilodeau, G. Instabilities in the Labrador Sea water mass structure during the last  
381 climatic cycle. *Can J Earth Sci* **37**, 795-809 (2000).

382 37 Stoner, J. S., Channell, J. E. T., Hillaire-Marcel, C. & Kissel, C. Geomagnetic paleointensity and  
383 environmental record from Labrador Sea core MD95-2024: global marine sediment and ice core  
384 chronostratigraphy for the last 110 kyr. *Earth and Planetary Science Letters* **183**, 161-177 (2000).

385 38 Conkright, M. E. *et al.* *World Ocean Database 2001*. Vol. 1 (U.S. Government Printing Office, 2002).

386 39 Hodell, D. A., Channell, J. E. T., Curtis, J. H., Romero, O. E. & Rohl, U. Onset of "Hudson Strait" Heinrich  
387 events in the eastern North Atlantic at the end of the middle Pleistocene transition (similar to 640 ka)?  
388 *Paleoceanography* **23**, doi:10.1029/2008PA001591 (2008).

389 40 Hodell, D. A., Evans, H. F., Channell, J. E. T. & Curtis, J. H. Phase relationships of North Atlantic ice-  
390 rafted debris and surface-deep climate proxies during the last glacial period. *Quaternary Science Reviews*  
391 **29**, 3875-3886, doi:10.1016/J.Quascirev.2010.09.006 (2010).

392 41 Shackleton, N. J., Hall, M. A. & Vincent, E. Phase relationships between millennial-scale events 64,000-  
393 24,000 years ago. *Paleoceanography* **15**, 565-569 (2000).

394 42 Skinner, L. C., Elderfield, H. & Hall, M. in *Ocean Circulation: Mechanisms and Impacts Geophysical*  
395 *Monograph Series* (eds A. Schmittner, J. Chiang, & S. Hemming) 197-208 (American Geophysical Union,  
396 2007).

397 43 Tjallingii, R. *et al.* Coherent high- and low-latitude control of the northwest African hydrological balance.  
398 *Nature Geoscience* **1**, 670-675, doi:Doi 10.1038/Ngeo289 (2008).

399 44 Zarriess, M. & Mackensen, A. Testing the impact of seasonal phytodetritus deposition on delta(13)C of  
400 epibenthic foraminifer *Cibicides wuellerstorfi*: A 31,000 year high-resolution record from the northwest  
401 African continental slope. *Paleoceanography* **26**, doi:10.1029/2010pa001944 (2011).

402 45 Zarriess, M. *Primary Productivity and Ocean Circulation Changes on orbital and millennial Timescales off*  
403 *Northwest Africa during the Last Glacial/Interglacial Cycle: Evidence from benthic foraminiferal*  
404 *Assemblages, stable carbon and oxygen isotopes and Mg/Ca Paleothermometry* Ph.D. thesis, Universitat  
405 Bremen, (2010).

406 46 Garcia, H. E. *et al.* *World Ocean Atlas 2009, Volume 4: Nutrients (phosphate, nitrate, silicate)*. (U.S.  
407 Government Printing Office, 2010).

408 47 Curry, W. B. & Oppo, D. W. Glacial water mass geometry and the distribution of d<sup>13</sup>C of SCO<sub>2</sub> in the  
409 western Atlantic Ocean. *Paleoceanography* **20**, PA1017, doi:10.1029/2004PA001021 (2005).

410  
411

412

413 Correspondence and requests for materials should be directed to Jean Lynch-Stieglitz

414

#### 415 **Acknowledgments**

416 The authors acknowledge the US National Science Foundation (OCE-0096472, OCE-0648258  
417 and OCE-1102743), a grant from the Comer Science and Education Foundation and a Rutt  
418 Bridges Undergraduate Research Fellowship to L.G.H. for funding this work. PC acknowledges  
419 the supports from the Natural Science Foundation of China (40921004 and 40930844). S.M. was  
420 funded through the DFG Research Center/Cluster of Excellence “The Ocean in the Earth  
421 System”. We also thank Tiee-Yuh Chang for technical assistance.

422

#### 423 **Competing Financial Interests**

424 The authors have no competing financial interest.

425

#### 426 **Contributions**

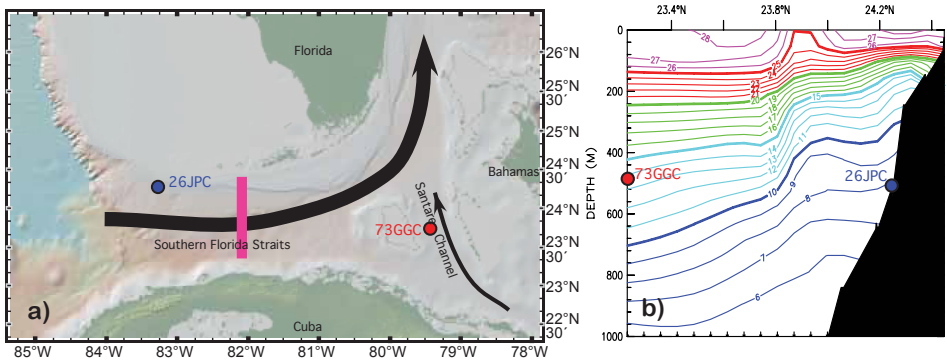
427 J.L.S., W.B.C., M.W.S. and L.G.H. collected and analyzed the sedimentary materials from  
428 KNR166-2, L.C.S. and S.M. contributed to the benthic carbon isotope compilation and P.C. and  
429 R.Z. contributed model output. All authors contributed to the interpretation of the data and  
430 model results and participated in the preparation of the manuscript.

431



432

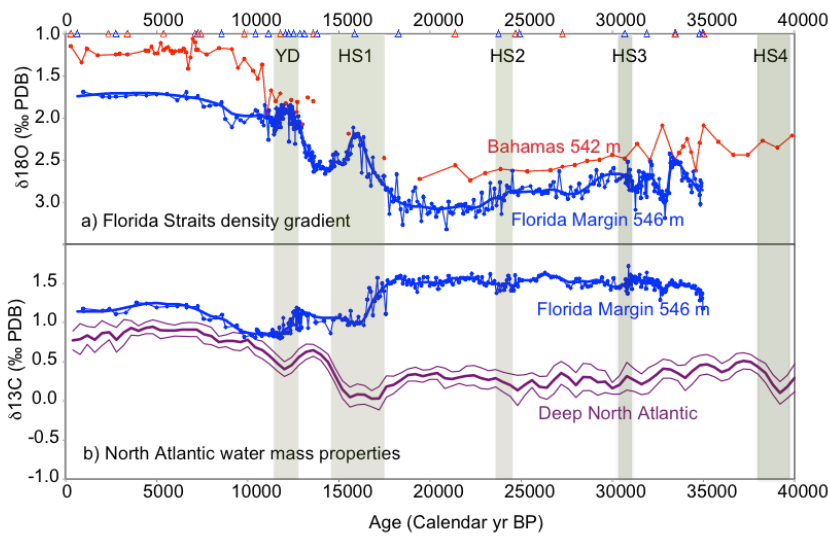
433 **Figures**



434

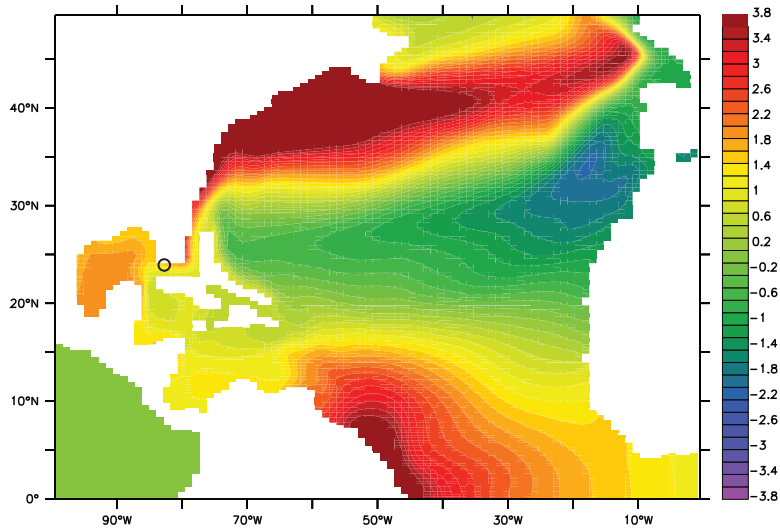
435

436 **Fig. 1. Core Locations and Context** a) Location of sediment cores for the data shown in  
437 Figure 2. The location of the temperature section shown in panel (b) is indicated with the pink  
438 line, and the approximate path of the Florida Current with the large black arrow. b) A North-  
439 south section of climatological temperature (°C) across the Florida Straits at 82° W, with the  
440 depth of the two sediment cores used to monitor the cross Straits density gradient indicated with  
441 circles<sup>38</sup>.

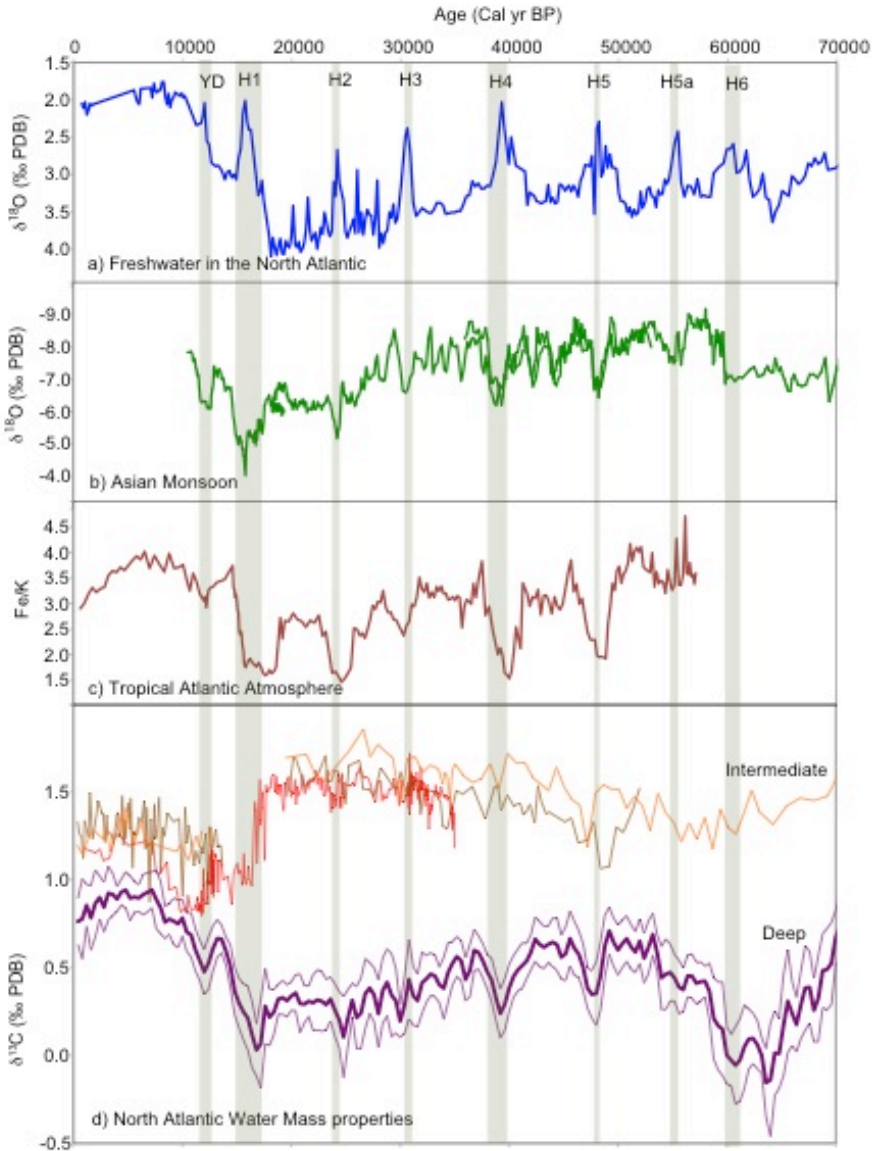


442

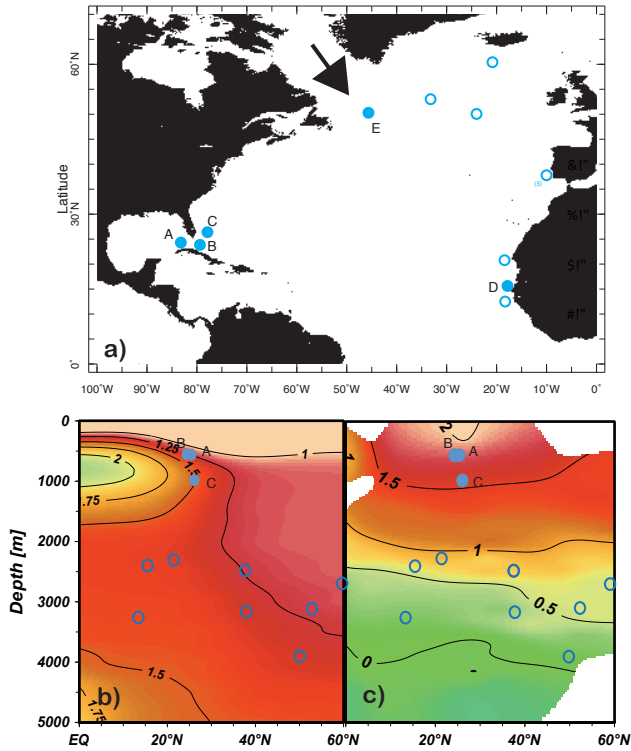
443 **Fig. 2. Glacial and Deglacial Records** a) Oxygen isotope ratio in benthic foraminifera from  
444 two cores on either side of the Florida Current (blue: KNR166-2-26JPC, red: KNR166-2-73GC,  
445 Locations shown on Figure 1). Depths of radiocarbon dates in these cores are indicated by  
446 triangles on the top axis. b) Carbon isotope ratios from the benthic foraminifera *Planulina*  
447 *ariminensis* from the same core on the Florida side of the Straits (blue: KNR166-2-26JPC,  
448 Location A on Figure 5), and average (800 year window) and +/- 2 standard error (purple) of  
449 eight high resolution *Cibicides wuellerstorfi*  $\delta^{13}\text{C}$  records from the deep Atlantic<sup>17,39-45</sup>.  
450 (Core Locations shown in Figure 5).



451  
 452 **Fig. 3. Modelled Temperature Anomaly** Temperature anomaly (K) at 579 m for water hosing  
 453 experiment (0.25 Sv) with LGM boundary conditions in CCSM3 (11 Sv AMOC reduction)<sup>24</sup>.  
 454 The location of KNR166-2-26JPC is indicated with a black circle.



455 **Fig. 4. Stage 3 Records** a) Oxygen isotope ratio in the planktonic foraminifera  
 456 *Neogloboquadrina pachyderma* (*l*) from the western North Atlantic <sup>36</sup>(Location E, Figure 5).  
 457 Low values reflect presence of glacial melt water. b) Oxygen isotope ratio in cave deposits in  
 458 China, reflecting changes in monsoon precipitation <sup>1</sup>. Green vertical bars extending through all  
 459 of the plots indicate the timing of the Younger Dryas and Heinrich stadials from this record. c)  
 460 The Fe/K ratio, an indicator of aridity in the West African Sahel (Location D, Figure 5) <sup>2</sup>. d)  
 461 Carbon isotope ratios in benthic foraminifera from intermediate waters (red: 546 m Location A  
 462 on Figure 5; orange: 542 m Location B on Figure 5) (this study) and (brown: 965 m Location C  
 463 in Figure 5) <sup>20</sup>. Average (800 year window) and +/- 2 standard error (purple) of seven high  
 464 resolution *Cibicides wuellerstorfi*  $\delta^{13}\text{C}$  records from the deep Atlantic <sup>17,39-45</sup>. (Locations in  
 465 Figure 5, Individual records in Supplemental Figure 2).



467  
 468 **Fig. 5. Location of other Records** a) Location of sediment cores for the data shown in Figures 2  
 469 and 3 (solid circles) and that contributed towards the deep North Atlantic  $\delta^{13}\text{C}$  averages (open  
 470 circles). The source of the Heinrich ice surges from the Hudson Straits is marked with an arrow.  
 471 b) Modern  $\text{PO}_4$  ( $\mu\text{mol kg}^{-1}$ ) distribution in the North Atlantic <sup>46</sup> with location of sediment cores  
 472 for the carbon isotope records shown in Figure 4 indicated with solid circles and those  
 473 contributing towards the deep North Atlantic  $\delta^{13}\text{C}$  averages with open circles. c) Glacial  $\delta^{13}\text{C}$   
 474 (‰ PDB) distribution in the North Atlantic <sup>47</sup>.  
 475